Journal of Medical Devices Technology
jmeditec.utm.my

Original Research

Performance Analysis of Wearable Antenna Worn in Close Proximity with Human Body

Faishal Adilah Suryanata[1], Naufal Fikri Muhammad[1], Nur Natasha Amyra Ahmad Azizi[1] , Raimi Dewan[1,2*] and Bappadittya Roy[3]

[1] *Advanced Radio Frequency & Microwave Research Group, Faculty of Electrical Engineering, Universiti Teknologi Malaysia, 81310 UTM Johor Bahru, Malaysia*
[2] *IJN-UTM Cardiovascular Engineering Centre, Universiti Teknologi Malaysia, 81310 UTM Johor Bahru, Malaysia.*
[3] *VIT-AP University, Amravati, Andhra Pradesh, India*

ARTICLE INFO

Article History:

Received 25 March 2023
Accepted 27 May 2023
Available online 30 May 2023

Keywords:
Wearable antenna,
S_{11} parameter,
Bending

ABSTRACT

In the healthcare applications, wearable technology is being rapidly developed. Electromagnetic wave will have an effect when the passive antennas is being closed to the human body because it will act as lossy medium. In this study, the effect of human tissue properties will be studied and will carry out under three conditions: (1) in free space, (2) on human tissue (chest body part) with and without airgap, (3) single and double bended condition of the antenna. The spacing gaps between the antenna and the human chest has been set up such as 2 mm, 4 mm, 6 mm. The bending radiuses for both single and double condition also being set up as 2 mm, 4 mm, 6 mm, 8 mm, 10 mm, and 12 mm. In this study, the effect of human body proximity and human body movement which caused bending to the wearable antenna are also analysed. It will be analysed using the CST Studio Suites 2021 Student Version software.

INTRODUCTION

A wearable antenna is a type of antenna which is applied onto human body and to be worn in short term or long term based on its intended usage (Rahayu and Kirana, 2021). A wearable antenna consists of basic construction of radiating patch, transmission feeding, a substrate, a grounded layer, and a feeding port. The wearable antenna is a part of body area network (BAN) system that found its application (but not limited to) in monitoring and detecting disease, and in health and wellness monitoring like in sports training (Hussain et al., 2018). The wearable antenna is subjected to performance degradation due to body proximity. It was also used as the Implantable Medical Devices (IMDs) that enlarged a variety of diagnostic and therapeutic functions including sensing, stimulation, monitoring, and during delivery. IMDs featuring antenna-enabled biotelemetry are essential for wireless communication with the environment, and this technology has sparked a lot of curiosity regarding the subject of antenna design and performance (Shah et al., 2019). Since the implantable medical devices is able to provide real-time monitor and diagnose while keep the mobility of the patients (Li et al., 2019). Wireless body area networks (WBANs) are a smart network integration that enables gadgets and sensors to collaborate to gather a number of key physiological parameters. WBANs are a well-established component of wearable consumer electronics (Berkelmann and Manteuffel, 2021; Dewan at al., 2022). The antenna efficiency that has low return loss and high gain may have a significant challenge. It happens because human body tissue can give an effect to the efficiency and the performance of the antenna. Bending condition of the wearable antenna due to the human body surfaces and movement may also give an effect to the antenna performance itself (Azizi, 2022). Therefore, the understanding of the effect of human body to the performance of wearable antenna is required, the difference performance between in free space condition and human body and the bending effect to the antenna performance is being studied in this paper. The design and the performance of the wearable antenna and the human body layer would be analyzed using the CST Studio Suites 2021 Student Version software. The S1,1

* Raimi Dewan (raimi.dar@utm.my)
Advanced Radio Frequency & Microwave Research Group, Faculty of Electrical Engineering, Universiti Teknologi Malaysia, 81310 UTM Johor Bahru, Malaysia

parameter or parameter sweep, and bending radius would be processed inside the CST process. Database of human body electrical properties would be used to design the human body layer.

MATERIAL AND METHODOLOGY

WEARABLE ANTENNA

Wearable Antenna is an antenna designed to be worn by the user which can be directly applied to the skin or over the clothing for transmission and receiving of wireless communication signals. Basic structure of an antenna consists of a radiating patch, a feeding port, feeding network, grounded layer, and a substrate. Figure 1 (a) and (b) shows the example of a wearable antenna design with its corresponding prototype in the subsequent Figure 1 (c) and (d). The conduction part of the antenna is made from nylon conductive fabric while the substrate is from a wool felt. Wearable antennas having to be worn by the user are subjected to the performance degradation due to human proximity. The parameter of performance for wearable antenna in terms of return loss, radiations pattern and gain will be covered in the following subsections. Figure 2 shows a wearable antenna which is mounted on human wrist.

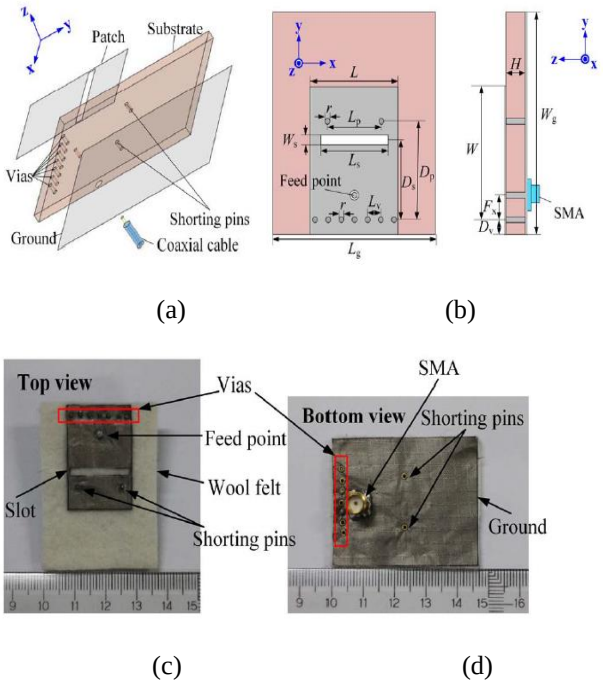

Fig 1 A (a) 3-Dimensional view and (b) top and side view of wearable antenna design. The (c) top and (d) bottom view of the fabricated wearable antenna for the corresponding design. (Lee et al., 2017).

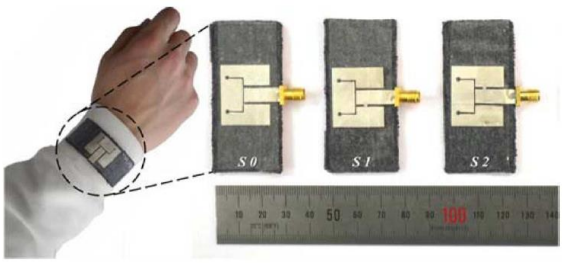

Fig 2 Wearable antenna on human wrist (Sang-Jun and Chang Won, 2011).

Return Loss

Return loss is a measure of the effectiveness of power deliverance from a specified transmission line to a load, which in this case, the load is an antenna (Alsager, 2011). Return loss equation is a negative of the reflection coefficient (S_{11}) as shown in equation 1 (Bird, 2009) where is ρ is a complex reflection coefficient. Figure 3 show a measurement result of an ultrawideband band-notched flexible antenna in free space and on-body condition. It can be observed that the reflection coefficient significantly experiences detuning due to the body proximity shown in blue line as opposed to the condition where the antenna is placed in the free space shown in red line. The reflection curve characteristics significantly changes when the antenna is placed onto human body as opposed to in free space condition. The substrate permittivity changes when the antenna is placed on the human body is one of the factors contributing to the detuning of the return loss curve characteristics. is one of the factors contribute to the detuning of the return ss curve characteristics.

$$Return\ Loss\ (RL) = -20\ \log_{10}|\rho| \quad (1)$$

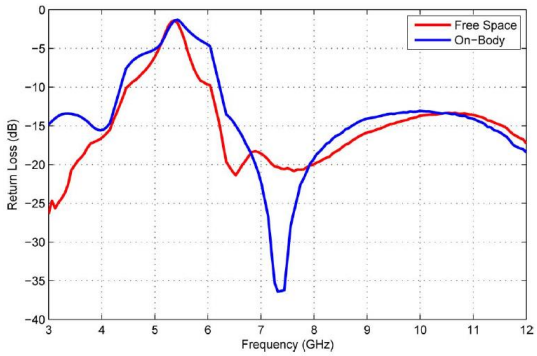

Fig 3 Reflection coefficient S_{11} measurement comparison in free space and On-body environment (Abbasi et al., 2013)

Radiation Pattern

Radiation pattern is another parameter performance of an antenna. Radiation pattern is the variation of power radiated as a function of direction and distance away from an antenna. The radiation pattern is also affected when in proximity with human bodies. In Abbasi et. Al., 2013, the antenna incorporated into a military beret for worn by military individuals or soldiers. Therefore, the antenna is very close to the human head based on its intended application. The simulation and measurement have been carried out to analyze the antenna radiation performance in the free space and human head phantom. The corresponding results are shown in Figure 4. It can be observed that the human proximity (represented by the human head phantom) does influence the radiation pattern of the antenna as opposed when it was place in free space. The back lobe radiation toward human head is more pronounced as compared to the antenna in free space subsequently decreasing the front to back lobe radiation of the antenna.

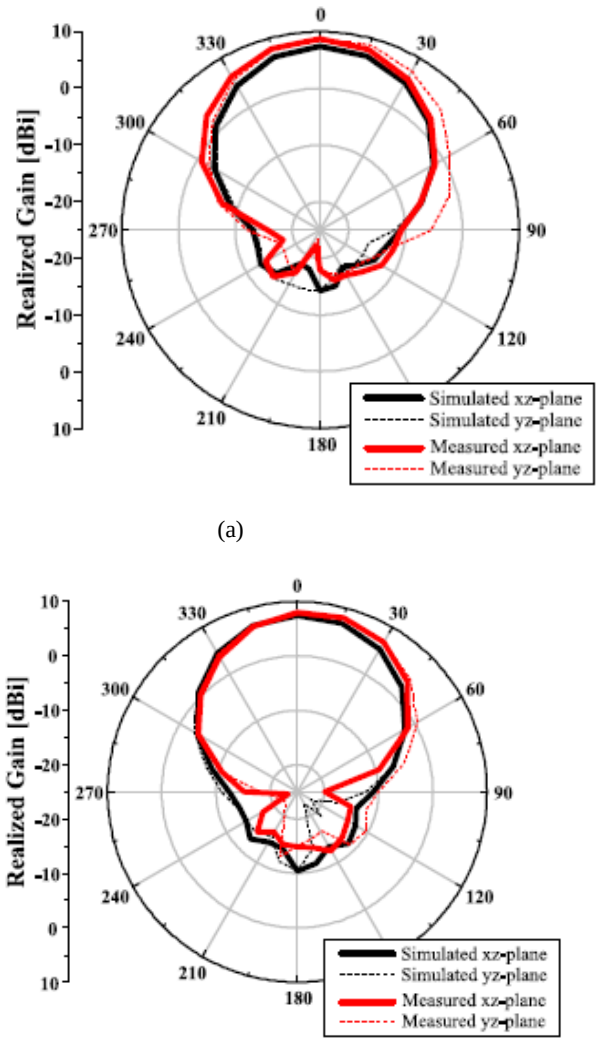

Fig 4 The simulated and measured radiation pattern of the antenna in the (a) Free space and (b) head phantom at 1.575 GHz (Rahayu and Kirana, 2021)

Gain

Gain is also a parameter that defines the performance of an antenna. Gain is a parameter describing how much of a power is transmitted in the direction of peak or maximum radiation in comparison to an isotropic antenna. Figure 5 shows the antenna radiation pattern results of the antenna in free space and on the skin equivalent phantom. It can be observed that the antenna on the human phantom shows higher maximum antenna gain as compared to the free space condition. The antenna is more directive when it is placed in close proximity to human phantom. The gain varies accordingly to the antenna height by a distance, d from the human phantom.

RESULTS AND DISCUSSION

Performance on Human Body Model

In Table 1, it defines the electrical properties data of chest layer that consists of the permittivity, conductivities, and thickness for modelling the human body that will be attached with the designed antenna. In Table 2, the average for the parameters is calculated and modelled as in Figure 6. In this study, it used the chest layer as the human body model and the antenna observed and simulated using the S_{11}parameter. S_{11}parameter itself is a power that reflected from the antenna to the source as the reflection coefficient (Dewan et al., 2022). The chest was chosen because of its larger and has non-curvy surface area as opposed to other human body surfaces making it suitable for the antenna to be attached on. On the chest, the antenna bending effect reduces the return loss and efficiency can be reduced.

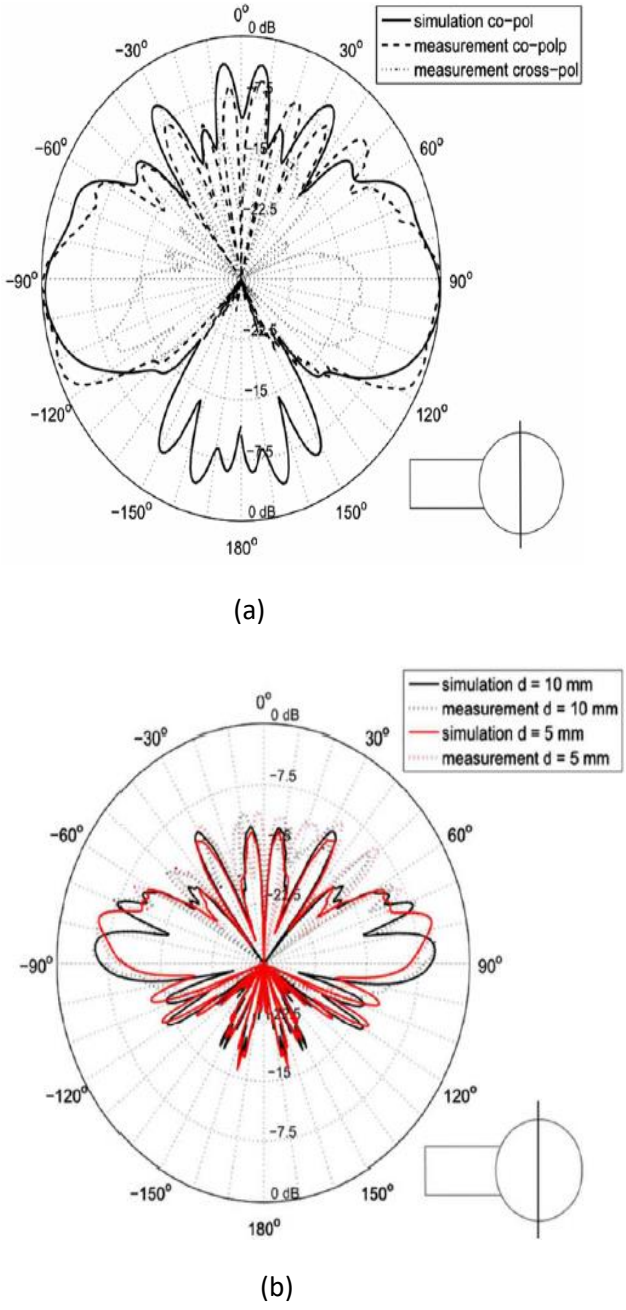

Fig 5 E-plane (xz-plane) (a) simulated and measured radiation pattern in free space (b) simulated and measured radiation pattern on the human phantom with varying distances of 5 mm and 10 mm (Puskely et al, 2015)

Table 1 Chest layer electrical properties (Azizi, 2022)

No.	Sub Body Part	Thickness	Permittivity	Conductivity	Sources
1.	Skin	2	36.06	2.84	
	Fat	4	5.03	0.23	(Nie et al., 2021)
	Muscle	5	49.84	3.93	
2.	Skin	2	35	3.8	
	Fat	5	4.95	0.3	(Bo Yin et al,, 2021)
	Muscle	20	48.4	5.12	
3.	Skin	1	49.90	-	
	Fat	5	5.58	-	(El May et al., 2021)
	Muscle	20	57.13	-	
4.	Skin	2	37.95	1.45	
	Fat	5	5.27	0.11	(Keshwani et al., 2021)
	Muscle	20	52.67	1.77	
5.	Skin	2	37.95	1.49	
	Fat	5	5.27	0.11	(Chengzhu Du et al,, 2021)
	Muscle	20	52.67	1.77	
6.	Skin	1	54.5	0.1	
	Fat	10	5.64	0.1	(Bouhassoune et al,, 2021)
	Muscle	60	54.5	0.6	
7.	Skin	2	37.95	1.49	
	Fat	5	5.27	0.11	(Amato et al, 2020)
	Muscle	20	52.67	1.77	

Table 2 Average of thickness, permittivity, and conductivity of chest electrical properties (Azizi, 2022)

Sub body part	Thickness	Permittivity	Conductivity
Skin	1.71	41.95	1.69
Fat	55.57	5.32	0.143
Muscle	26.43	50.74	2.21

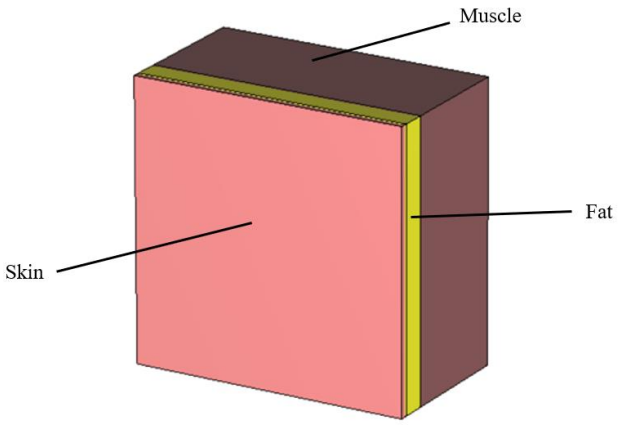

Figure 6 Chest layer body model (Azizi, 2022)

Free Space

Free space is an empty environment where the antenna is being located and influenced by the earth surface. The frequency range of the antenna is being referred to the bandwidth for the optimum levels. It can be taken at $S_{11} \leq$10dB that can be denoted in the 90% of the input power with 10% power loss reflected to the source. From the simulation graph in Figure 7, it obtained 60 MHz as a bandwidth, 2.37 GHz as a lower frequency and high frequency at 2.43 GHz. Inside the graph and being illustrated in the Table 1.3, it also provides return loss at -40.04 dB with realized gain at 5.28 dBi and 74.54% as total efficiency at resonant frequency at 2.4 GHz. In Figure 8, it shows the parameter sweeps of the inset width. The inset length variation and reflection coefficient which is S_{11} that is operate at 2.4 GHz justified by $S_{11} \leq$15dB is shown in Figure 9. The inset itself is for matching the impedance between the transmission feeding network and radiating patch. The optimum parameter of S_{11} can be get by adjusting the value of inset width and length of the antenna. It also shown that the resonant frequency is increased to 2.40 GHz and -40.04 dB as a return loss. From the inset width and length figure, it can be concluded that the best value of 3.07 mm and 8.54 mm.

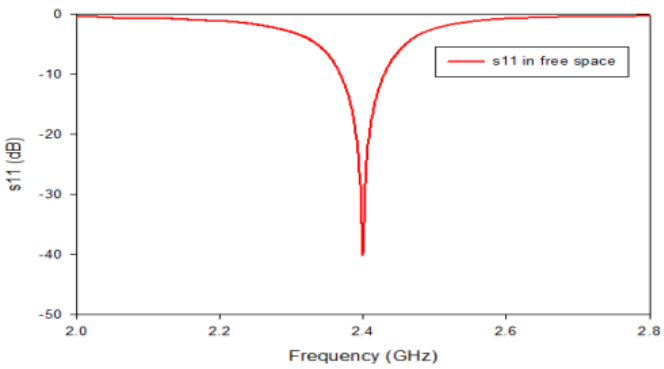

Fig 7 S_{11} in free space (Azizi, 2022)

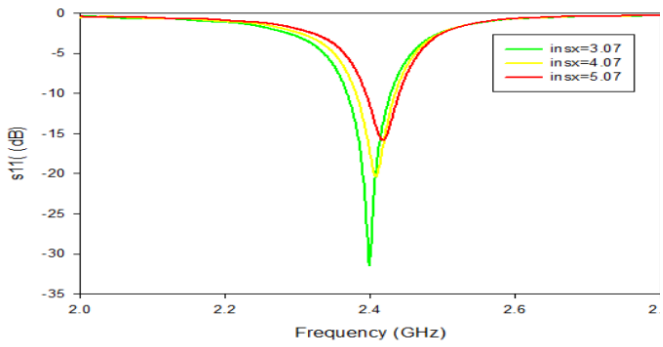

Fig 8 Parameter sweeps of the inset width (Azizi, 2022)

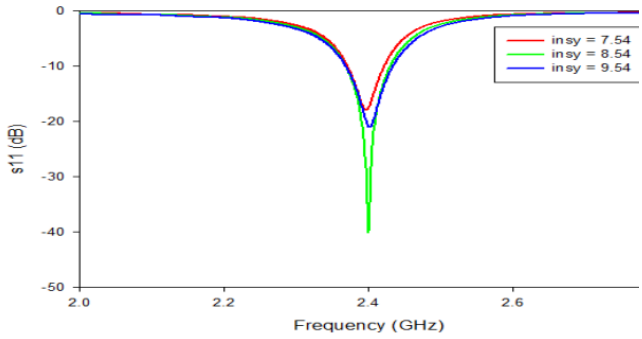

Fig 9 Parameter sweeps for inset length variation (Azizi, 2022)

Table 3 Parameters list and values in free space

Parameter	Obtained Value
Frequency (GHz)	2.40
Return loss (dB)	-40.04
Realized gain (dBi)	5.28
Total efficiency (%)	74.54

On Human Tissue Layers

On human tissue layers, the resonant frequency of the antenna is shifted to 2.67 GHz with frequency detuning of 11.25% as compared to the antenna in free space. The performance characteristics of the antenna is being influence by the human tissue properties including the S_{11} (dB), realized gain (dBi), and radiation pattern. The inset width and length are being modified by shifting the S_{11} curve into 2.40 GHz and slightly increases compared to in free space. Figure 10 shows the parameter sweeps for inset width with the value of inset feed is 3.20 mm and the parameter sweeps for length of patch antenna with the value of 35.05 mm shown in Figure 11. It is shown that both inset width is being increased from 35.05 mm to 35.20 mm with the length of patch antenna increased from 35.00 mm to 35.10 mm and a step size of 0.05 mm. In Figure 12, the S_{11} result have an airgap of 0,2,4 and 6 mm. The ratio of two separate resonant frequencies will be decreased when the airgap itself is increases. The different in the depth of the return loss is resulted from the different airgap and it is shown in Table 4.

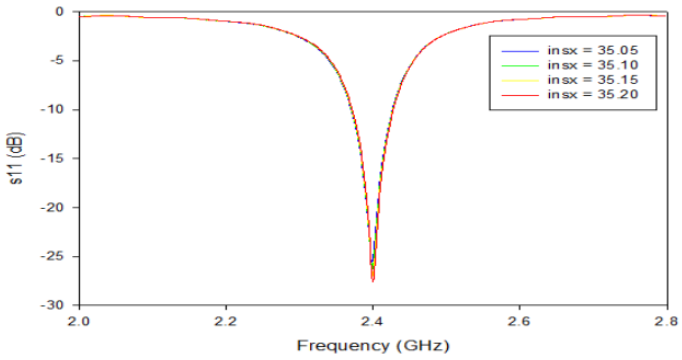

Fig 10 Parameter sweeps for width of inset feed (Azizi, 2022)

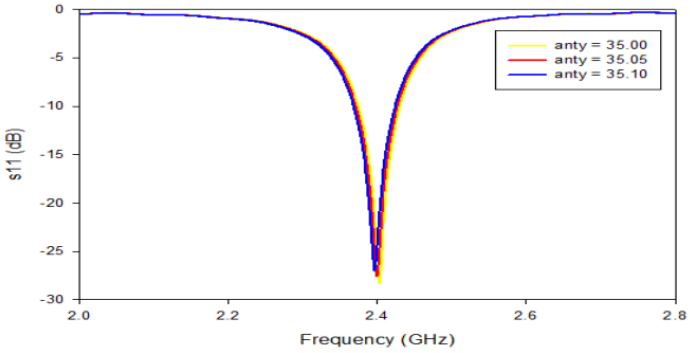

Fig 11 Parameter sweeps for inset length variation (Azizi, 2022)

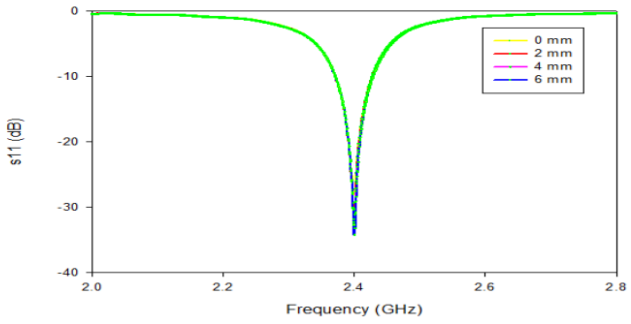

Fig 12 S_{11} antenna with airgaps (Azizi, 2022)

Table 4 The S_{11} values for each airgap at 2.40 GHz (Azizi, 2022)

Airgaps (mm)	Reflection coefficient, S_{11} (dB)	Reflection coefficient, S_{11}different (dB)
0	-28.08	0.00
2	-30.37	-2.29
4	-32.39	-2.02
6	-34.28	-1.89

Bending

S_{11} results of 0 mm (without bending), 2 mm, 4 mm, 6 mm, 8 mm, 10 mm, and 12 mm is shown in Figure 13. The bending radius of the S_{11}curve is being shifted to the left and upward and the characteristics curve of S_{11} is maintained can be called as double bending condition. The curve is being increased from -40.04 dB to -13.34 dB the bending of antenna is becoming more apparent.

In Figure 14, S_{11} result of without bending and all bending radiuses such as 2 mm, 4 mm, 6 mm, 8 mm, 10 mm, and 12 mm. The S_{11} curve for 2 mm, 4 mm, and 6 mm is being shifted into the left and the curve for 8 mm, 10 mm, and 12 mm shifted to the right. When the bending radius is increased, all the S_{11} curve at different bending radius is not shifted at the same direction. It decreased the effective length and shift the resonant frequency to become higher.

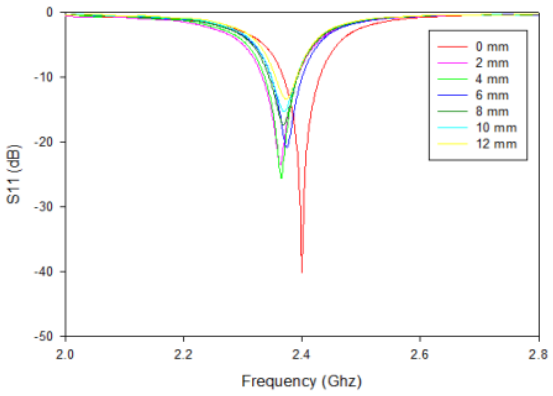

Fig 13 Double bend antenna of S_{11} (Azizi, 2022)

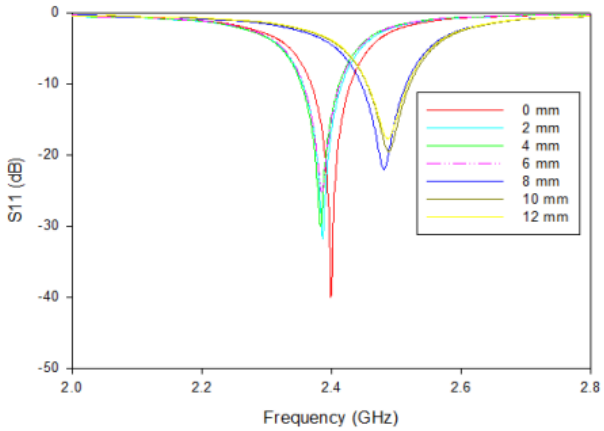

Fig 14 Single bend antenna of S_{11} (Azizi, 2022)

CONCLUSION

The antenna performance parameters such as reflection parameters such as reflection coefficient (S_{11}), bandwidth, realized gain (dBi), total efficiency, and radiation pattern is being shown can be affected by the high dielectric of the human tissue. In this study, the spacing gap is created between the modelled antenna of chest tissue to study the performance of the antenna between different distances. It shows that the further gap will resulting the better S_{11}, realized gain, and radiation pattern. The single and double bending radius of the antenna also being created and the S_{11} results can be decrease when the antenna is having too much bending. It shows that the single bend has more minor frequency detuning rather than the double bend.

Acknowledgment

The authors would like to thank the Ministry of Higher Education (MOHE), School of Postgraduate Studies (SPS), Research Management Centre, Advanced Diagnostics and Progressive Human Care Research Group, Faculty of Electrical Engineering and Universiti Teknologi Malaysia (UTM), Johor Bahru, for the support of the research under UTM Encouragement Research Grant Q.J130000.3851.20J74.

REFERENCES

Abbasi, Q. H., Rehman, M. U., Yang, X., Alomainy, A., Qaraqe, K., Serpedin, E. 2013. Ultrawideband Band-Notched Flexible Antenna for Wearable Applications. IEEE Antennas and Wireless Propagation Letters, 12, 1606-1609.

Alsager, A. F. (2011). Design and Analysis of Microstrip Patch Antenna Arrays. (Msc. Thesis). University College of Borås.

Amato, F., Occhiuzzi, C.. Marrocco, G. 2020. Epidermal Backscattering Antennas in the 5G Framework: Performance and Perspectives. IEEE Journal of Radio Frequency Identification, 4(3), 176-185.

Azizi, N. N. A. A. 2022. Wearable 2.4 GHz Microstrip Patch Antenna on Poly Lactic Acid Substrate For Biomedical Telemetry Application. (Bachelor of Engineering (Bio-Medical)). Universiti Teknologi Malaysia,

Berkelmann, L., Manteuffel, D. 2021. Antenna Parameters for On-Body Communications With Wearable and Implantable Antennas. IEEE Transactions on Antennas and Propagation.

Bird, T. S. 2009. Definition and Misuse of Return Loss [Report of the Transactions Editor-in-Chief]. IEEE Antennas and Propagation Magazine, 51(2), 166-167.

Bouhassoune, I., Chaibi, H., Chehri, A. and Saadane, R., 2021. UHF RFID Spiral-Loaded Dipole Tag Antenna Conception for Healthcare Applications. Procedia Computer Science, 192(2021), 2531-2539.

Bo Yin, M. Y., Youhai Yu. 2021. A Novel Compact Wearable Antenna Design for ISM Band. Progress in Electromagnetics Research C, 107(97-111).

Chengzhu Du, X. W., Gaoya Jin, Shunshi Zhong. 2021. A Compact Tri-Band Flexible MIMO Antenna Based on Liquid Crystal Polymer for Wearable Applications. 102, 217-232.

Dewan, R., Yusri, N. and Salim, M.I.M., 2022. Reduced-size Biocompatible Implantable Planar Inverted F-Antenna. Elektrika Journal of Electrical Engineering, 21(3), 62-68.

El May, W., Sfar, I., Ribero, J. M., Osman, L. 2021. Design of Low-Profile and Safe Low SAR Tri-Band Textile EBG-Based Antenna for IoT Applications. Prog. Electromagn. Res. Lett., 98, 85-94.

Hussain, S., Hafeez, S., Memon, S.A. and Pirzada, N. 2018. Design of Wearable Patch Antenna for Wireless Body Area Networks. (IJACSA) Internnational Journal of Advanced Computer Science and Applications, 9(9).

Keshwani, V.R., Bhavarthe, P.P. and Rathod, S.S., 2021. Eight Shape Electromagnetic Band Spacing gap Structure for Bandwidth Improvement of Wearable Antenna. Progress In Electromagnetics Research C, 116, 37-49.

Lee, H., Tak, J., Choi, J. 2017. Wearable Antenna Integrated into Military Berets for Indoor/Outdoor Positioning System. IEEE Antennas and Wireless Propagation Letters, 16, 1919-1922.

Li, H., Wang, B., Guo, L., Xiong, J. 2019. Efficient and Wideband Implantable Antenna Based on Magnetic Structures. IEEE Transactions on Antennas and Propagation, 67(12), 7242-7251.

Nie, H.-K., Xuan, X.-W., Ren, G.-J. 2021. Wearable antenna pressure sensor with electromagnetic bandgap for elderly fall monitoring. AEU - International Journal of Electronics and Communications, 138.

Puskely, J., Pokorny, M., Lacik, J., Raida, Z. 2015. Wearable Disc-Like Antenna for Body-Centric Communications at 61 GHz. IEEE Antennas and Wireless Propagation Letters, 14, 1490-1493.

Rahayu, Y. and Kirana, T., 2021. Flexible Multi-Layer Condura Fabric Ultra Wide-Band Antenna For Telemedicine Application. In *2021 9th International Conference on Information and Communication Technology (ICoICT)* (pp. 133-137). IEEE.

Sang-Jun, H., Chang Won, J. 2011. Reconfigurable Beam Steering Using a Microstrip Patch Antenna With a U-Slot for Wearable Fabric Applications. IEEE Antennas and Wireless Propagation Letters, 10, 1228-1231.

Shah, I. A., Zada, M., Yoo, H. 2019. Design and Analysis of a Compact-Sized Multiband Spiral-Shaped Implantable Antenna for Scalp Implantable and Leadless Pacemaker Systems. IEEE Transactions on Antennas and Propagation, 67(6), 4230-4234.